

Filtered asymmetric dark matter during the Peccei-Quinn phase transition

Moslem Ahmadvand

Institute for Research in Fundamental Sciences (IPM)
ahmadvand@ipm.ir

- Dark matter problem
- Strong CP problem and the Peccei-Quinn (PQ) solution
- The QCD axion model
- PQ phase transition
- Dark matter relic abundance
- Effective couplings of the axion
- Gravitational waves
- Effective dark matter interactions

Dark matter problem

- Astrophysical and cosmological observations support the existence of dark matter (DM).
- The nature of DM in fundamental physics is unknown...

Some of mechanisms to explain the DM relic abundance:

- Thermal WIMP paradigm
- Non-thermal DM models
- Asymmetric DM models
- Filtered DM: DM dynamically acquires a mass and its number density is abruptly frozen out. The mechanism provides a framework to evade the Griest-Kamionkowski (GK) bound on the mass of thermally produced DM.

A filtered asymmetric DM scenario is proposed.

- A QCD axion model as a solution of the strong CP problem is used.
- RH neutrinos become massive into the bubbles of the new phase and heavy DMs can be generated.
- To obtain the DM relic abundance, the scenario is not restricted to $m_{DM} \gg T_n$.
- First-order PQ phase transition leads to the bubble nucleation.
- Lepton number violating interactions along with CP violating effects during the phase transition are considered.

Strong CP problem and the PQ solution

- For vanishing quark masses, particularly for u and d quarks, strong interactions are approximately invariant under the global flavor transformation $U(2)_V \times U(2)_A$.
- There are not four pseudo Nambu-Goldstone bosons due to quark condensates since $U(1)_A$ is in fact anomalous.
- Due to the triangle diagram and QCD vacuum structure

$$\partial_\mu J_5^\mu = \frac{-g^2}{16\pi^2} G_a^{\mu\nu} \tilde{G}_{a\mu\nu} \quad (1)$$

which affects the QCD Lagrangian

$$S_{\text{eff}} = S_{\text{QCD}} + \theta \frac{g^2}{32\pi^2} \int d^4x G_a^{\mu\nu} \tilde{G}_{a\mu\nu} \quad (2)$$

- The θ -term violates CP.

Strong CP problem and the PQ solution

- This term contributes to the neutron electric dipole moment, $d_n \approx 3.6 \times 10^{-16} \bar{\theta} e \text{ cm}$, which is experimentally constrained $|d_n| < 2.9 \times 10^{-26} e \text{ cm}$ (90% C.L.) and thereby $\bar{\theta} \lesssim 10^{-10}$.
- The strong CP problem: there is no reason in the SM why $\bar{\theta}$ should be very small.
- An interesting solution to this problem is based on a global chiral $U(1)_{\text{PQ}}$ symmetry proposed by Peccei and Quinn.
- At QCD scales, the interaction of a pseudo-scalar field, the axion a , is effectively added to the Lagrangian, $(a/f_a + \bar{\theta}) G \tilde{G}$.
- The CP-violating term can be cancelled via the vacuum expectation value (vev) of axion at the minimum of its potential, addressing the strong CP problem.

Strong CP problem and the PQ solution

- The UV completion of such non-renormalizable interactions can be constructed in a model invariant under $U(1)_{PQ}$.
- At some high energy scale, the symmetry is spontaneously broken and the resulting pseudo-Nambu Goldstone boson would be matched with the axion.

Two types of axion models can be categorized:

- 1 Kim-Shifman-Vainshtein-Zakharov (KSVZ) models which contain extra heavy quarks and PQ scalar fields, carrying the PQ charge
- 2 Dine-Fischler-Srednicki-Zhitnitsky (DFSZ) models in which beside the PQ scalar field, an additional Higgs field is introduced

Model

The Lagrangian of the model:

$$\mathcal{L} \supset |\partial_\mu \Phi|^2 + V(\Phi, H_u, H_d) + \bar{N}_{R_i} i \partial_\mu N_{R_i} + y_{ij} \Phi \bar{N}_{R_i} N_{R_j}^c \quad (3)$$

where

$$\begin{aligned} V(\Phi, H_u, H_d) = & \lambda_\phi (|\Phi|^2 - v_\phi^2/2)^2 + |H_d|^2 (\kappa_d |\Phi|^2 - \mu_d^2) \\ & + |H_u|^2 (\kappa_u |\Phi|^2 + \mu_u^2) - (\kappa \Phi^\dagger H_u H_d + h.c.) + \lambda_d |H_d|^4 \\ & + \lambda_u |H_u|^4 + \lambda_1 |H_u H_d|^2 + \lambda_2 |H_u|^2 |H_d|^2 \end{aligned} \quad (4)$$

The Yukawa interaction violates the lepton number by two units $\Delta L = 2$ in case $L(N_{R_i}) = 1$.

$$y_u \bar{Q}_L H_u u_R + y_d \bar{Q}_L H_d d_R + y_l \bar{\Psi}_{L_i} H_d l_R + y_{N_\alpha} \bar{\Psi}_{L_i} \tilde{H}_d N_{R_\alpha} + h.c.. \quad (5)$$

- The Lagrangian should be invariant under $U(1)_{PQ}$. PQ invariance of $\Phi^\dagger H_u H_d$ implies $X_{H_u} + X_{H_d} = X_\Phi$.
- Imposing the orthogonality between PQ and corresponding hypercharge currents, $-X_{H_u} v_u^2 + X_{H_d} v_d^2 = 0$, defining $v_u = v \sin \theta$ and $v_d = v \cos \theta$, and choosing $X_\Phi = 1$, we may determine all charges through

$$X_{H_d} = \sin^2 \theta, \quad X_{H_u} = \cos^2 \theta, \quad (6)$$

- The SM Higgs is indeed $H = H_d \cos \theta + \tilde{H}_u \sin \theta$, where $\tilde{H}_u = i\sigma_2 H_u^*$, and $v^2 = v_d^2 + v_u^2$.
- The PQ symmetry is spontaneously broken by the vev of Φ , such that $\Phi = 1/\sqrt{2}(\phi + f_a) \exp(ia/f_a)$ and the axion field is shifted by the PQ transformation.

Field	$SU(3)_c$	$SU(2)_L$	$U(1)_Y$	$U(1)_{PQ}$
Φ	1	1	0	1
H_u	1	2	$-\frac{1}{2}$	$\cos^2 \theta$
H_d	1	2	$\frac{1}{2}$	$\sin^2 \theta$
Q_L	3	2	$\frac{1}{6}$	$\cos^2 \theta$
u_R	3	1	$\frac{2}{3}$	0
d_R	3	1	$-\frac{1}{3}$	$2\cos^2 \theta - 1$
Ψ_L	1	2	$-\frac{1}{2}$	$\frac{1}{2} - \sin^2 \theta$
e_R	1	1	-1	$\frac{1}{2} - 2\sin^2 \theta$
N_R	1	1	0	$\frac{1}{2}$

Table: Charge assignment and group representation of the fields in the model

The potential in terms of electrically neutral components at the tree-level:

$$\begin{aligned}
 V = & \frac{\lambda_\phi}{4} (\phi^2 - f_a^2)^2 + \frac{1}{2} h_d^2 \left(\frac{\kappa_d}{2} \phi^2 - \mu_d^2 \right) + \frac{1}{2} h_u^2 \left(\frac{\kappa_u}{2} \phi^2 + \mu_u^2 \right) - \frac{\kappa}{\sqrt{2}} \phi h_u h_d \\
 & + \frac{\lambda_d}{4} h_d^4 + \frac{\lambda_u}{4} h_u^4 + \frac{\lambda_1 + \lambda_2}{4} h_u^2 h_d^2.
 \end{aligned} \tag{7}$$

Assuming the case in which h_u vanishes during the PT, there are two minima: 1- ($\phi = f_a$, $h_d = h_u = 0$) and 2- ($h_d = \mu_d^2/\lambda_d$, $\phi = h_u = 0$). For this PT, we study the first direction.

To account for quantum and thermal effects on the potential, we obtain the one-loop effective potential at finite temperature containing the resummed daisy (ring) diagrams,

$$V_t = V + V_{\text{CW}} + V_{\text{th}} + V_r \tag{8}$$

PQ phase transition

The one-loop Coleman-Weinberg quantum correction:

$$V_{\text{CW}}(\phi) = \sum_i (-1)^{F_{b/f}} g_i \frac{m_i^4(\phi)}{64\pi^2} \left[\ln \left(\frac{m_i^2(\phi)}{\Lambda^2} \right) - c_i \right]. \quad (9)$$

The one-loop thermal correction:

$$V_T(\phi, T) = \sum_i (-1)^{F_{b/f}} g_i \frac{T^4}{2\pi^2} J_{b/f} \left[\frac{m_i^2(\phi)}{T^2} \right] \quad (10)$$

where

$$J_{b/f}(y^2) = \int_0^\infty dx x^2 \ln \left[1 \mp e^{-\sqrt{x^2+y^2}} \right] \quad (11)$$

The daisy (ring) diagram contribution:

$$V_r(\phi, T) = - \sum_{i \in b} \frac{g_i T}{12\pi} \left([m_i^2(\phi) + \Pi_i(T)]^{3/2} - [m_i^2(\phi)]^{3/2} \right) \quad (12)$$

Thermal mass squared of the scalars:

$$\Pi_{\phi}(T) = \frac{T^2}{6} (\kappa_d + \kappa_u + 2\lambda_{\phi}), \quad (13)$$

$$\Pi_{h_d}(T) = \frac{T^2}{48} \left(9g^2 + 3g'^2 + \frac{12\lambda_t^2}{\cos^2 \theta_w} + 24\lambda_d + 4\kappa_d + 8\lambda_1 + 8\lambda_2 \right), \quad (14)$$

$$\Pi_{h_u}(T) = \frac{T^2}{48} (9g^2 + 3g'^2 + 24\lambda_u + 4\kappa_u + 8\lambda_1 + 8\lambda_2). \quad (15)$$

For some representative values of parameters, e.g., $y_1 = \sqrt{2}$, $y_2 = \sqrt{2}/2$, $y_3 = \sqrt{2} \times 10^{-3}$, $\kappa_u = 3$, $\lambda_u = \lambda_d = \lambda_1 = \lambda_2 = 10^{-2}$, $\kappa_d < \lambda_{\phi} = 10^{-8}$, and $f_a = 100 \text{ PeV}$, we find the PQ PT is of first order and the two degenerate phases are separated through a barrier at the critical temperature.

PQ phase transition

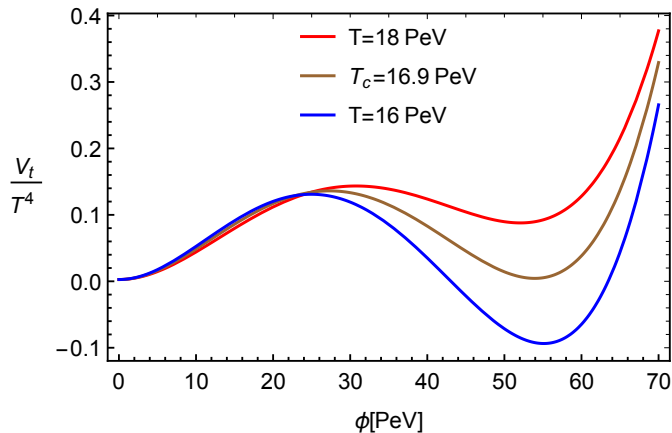


Figure: For $f_a = 100$ PeV, the total potential at three different temperatures is displayed.

the three-dimensional Euclidean bounce action:

$$S_3(T) = \int_0^\infty 4\pi r^2 dr \left[\frac{1}{2} \left(\frac{d\phi}{dr} \right)^2 + V_t(\phi, T) \right]. \quad (16)$$

By extremizing the action, we obtain the bounce equation and according to the following boundary condition, the equation can be numerically solved

$$\frac{d^2\phi}{dr^2} + \frac{2}{r} \frac{d\phi}{dr} = \frac{\partial V_t}{\partial \phi}, \quad \left. \frac{d\phi}{dr} \right|_{r=0} = 0, \quad \phi(\infty) = 0. \quad (17)$$

Bounce solution

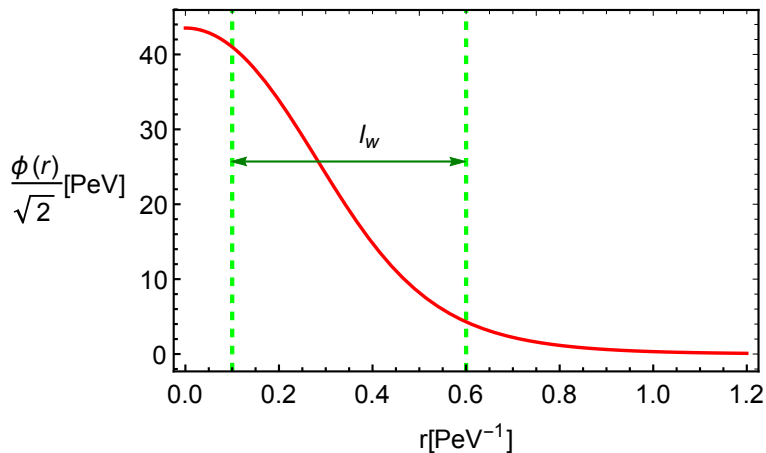


Figure: The bubble profile as the solution of the bounce equation is shown. l_w denotes the wall width.

Nucleation temperature

Bubbles nucleate when the bubble formation probability, proportional to $\exp(-S_3(T)/T)$, is of the order of one. Therefore, we can find the nucleation temperature, T_n , by the following relation

$$\frac{S_3(T_n)}{T_n} = 4 \ln \left(\frac{T_n}{H_*} \right), \quad (18)$$

As a result, using the obtained solution, we find the nucleation temperature of the PT, $T_n \simeq 9.19 \text{ PeV}$.

Boltzmann equation

The Liouville operator of phase space distribution function f_N for DMs in the wall frame:

$$\mathbf{L}[f_N] = \frac{df_N}{dt} = \frac{p_z}{E} \frac{\partial f_N}{\partial z} + F \frac{\partial f_N}{\partial p_z}. \quad (19)$$

F is the semiclassical force

$$F = -\frac{m_N(z)}{E} \frac{\partial m_N}{\partial z} \pm s \frac{m_N(z)}{EE_z} \left(\frac{\partial m_N}{\partial z} \frac{\partial \theta}{\partial z} + \frac{m_N(z)}{2} \frac{\partial^2 \theta}{\partial z^2} - \frac{m_N^2(z)}{2E^2} \frac{\partial m_N}{\partial z} \frac{\partial \theta}{\partial z} \right) \quad (20)$$

CP-violating sources are originated from the complex mass term

$$\hat{m}_N(z) = y_i \phi(z) / \sqrt{2} \exp[i\theta(z)] = m_N(z) \exp[i\theta(z)]. \quad (21)$$

$$\phi(z) = \frac{A}{2} (1 + \tanh[Bz]) \quad (22)$$

$$\theta(z) = \arctan \left(\frac{\Delta\theta}{2} \left[1 + \tanh\left(\frac{z}{l_w}\right) \right] \right). \quad (23)$$

Boltzmann equation

Using the ansatz $f_N = \mathcal{A}(z, p_z) \exp(-E^P/T)$ for the distribution function, we describe the deviation from equilibrium by \mathcal{A} which also includes the chemical potential.

Integrating over p_x and p_y , for RH chirality the Liouville operator would be

$$g_N \int \frac{dp_x dp_y}{(2\pi)^2} \mathbf{L}[f_N] \sim \left[\left(\frac{p_z}{m_N} \frac{\partial}{\partial z} - \left(\frac{\partial m_N}{\partial z} \pm \left(\frac{1}{2m_N} \frac{\partial m_N}{\partial z} \frac{\partial \theta}{\partial z} + \frac{1}{2} \frac{\partial^2 \theta}{\partial z^2} \right) \right) \frac{\partial}{\partial p_z} - \left(\frac{\partial m_N}{\partial z} \right) \frac{v_w}{T} \right) \mathcal{A}_{\pm}(z, p_z) \right] \frac{g_N m_N T}{2\pi} \exp \left(\frac{v_w p_z - \sqrt{m_N^2 + p_z^2}}{T} \right) \quad (24)$$

Boltzmann equation

According to the Boltzmann equation, $\mathbf{L}[f_N] = \mathbf{C}[f_N]$. The integration over the collision term is

$$g_N \int \frac{dp_x dp_y}{(2\pi)^2} \mathbf{C}[f_N] = -g_N^2 [\mathcal{A}_\pm(z, p_z) - 1] \\ \times \int \frac{dp_x dp_y}{(2\pi)^2} \frac{d^3 q}{2E_p^p (2\pi)^3 2E_q^p} 4\tilde{F}\sigma \exp\left(-\frac{E_p^p + E_q^p}{T}\right) \quad (25)$$

where σ is the spin-averaged cross section of such processes

$$N_R(p^p) + N_R(q^p) \rightarrow \phi(k^p) + \phi(l^p) \quad (26)$$

and

$$\tilde{F} = \sqrt{((p+q)^2 - 2m_N^2)^2 - 4m_N^4}/2 \quad (27)$$

One can rewrite the equation as

$$a_{\pm}(z, p_z) \frac{\partial \mathcal{A}_{\pm}}{\partial z} + b_{\pm}(z, p_z) \frac{\partial \mathcal{A}_{\pm}}{\partial p_z} = c_{\pm}(\mathcal{A}_{\pm}, z, p_z) \quad (28)$$

where

$$\frac{dz(\lambda)}{d\lambda} = a_{\pm}(z, p_z), \quad \frac{dp_z(\lambda)}{d\lambda} = b_{\pm}(z, p_z) \quad (29)$$

$$\frac{d\mathcal{A}_{\pm}(z(\lambda), p_z(\lambda))}{d\lambda} = c_{\pm}(\mathcal{A}_{\pm}(\lambda), z(\lambda), p_z(\lambda)) \quad (30)$$

and λ parameterizes a given curve on the (z, p_z) plane.

Solution

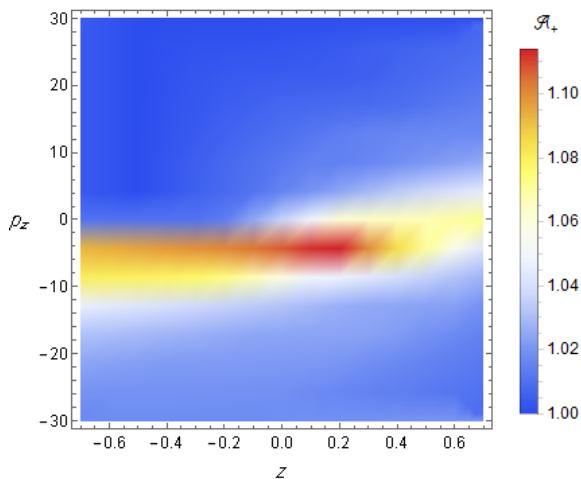


Figure: For two bubble velocities, $v_w = 0.01$, the factor \mathcal{A}_+ for DM particles is displayed. Since to obtain the observed relic abundance, it requires $\Delta\theta \ll 1$ and hence since \mathcal{A}_+ and \mathcal{A}_- are displayed almost the same, \mathcal{A}_+ is only shown.

Integrating over p_z at deep inside the bubble, we obtain the net number density $\Delta n_N/T_n^3$ in T_n units.

The DM relic abundance in the asymmetric case:

$$h^2\Omega_{\text{DM}} \simeq \frac{m_N^{\text{in}} \Delta n_N g_{*0} T_0^3}{3M_{\text{pl}}^2 (H_0/h)^2 g_* T_n^3} \quad (31)$$

the observed relic abundance, $h^2\Omega_{\text{DM}} \simeq 0.12$, can be obtained for, e.g., $y_1 = \sqrt{2}$ or $m_N^{\text{in}} \simeq 66.3 \text{ PeV}$ and from the attained $\Delta n_N/T_n^3$ which is determined by $\Delta\theta \sim 10^{-12}$.

Phenomenology, axion couplings

Due to the spontaneous PQ symmetry breaking, the effective interactions of the axion are expressed as

$$\mathcal{L}_a \supset \frac{g_s^2}{32\pi^2 f_a} a G \tilde{G} + \frac{g_{a\gamma}}{4} a F \tilde{F} - \frac{c_f^0}{2f_a} \partial_\mu a \bar{f} \gamma^\mu \gamma_5 f - \frac{c_{N_R}^0}{2f_a} \partial_\mu a \bar{N}_R \gamma^\mu N_R \quad (32)$$

where

$$g_{a\gamma} = \frac{e^2}{8\pi^2 f_a} \frac{\mathcal{E}}{\mathcal{N}} - \frac{e^2}{8\pi^2 f_a} \left(\frac{2}{3} \frac{4m_d + m_u}{m_d + m_u} \right) \quad (33)$$

$$c_f^0 = \frac{X_{f_R} - X_{f_L}}{2\mathcal{N}} = \frac{X_{H_f}}{2\mathcal{N}}, \quad c_{N_R}^0 = \frac{X_\Phi}{2\mathcal{N}} \quad (34)$$

$$\mathcal{N} = \frac{n_g}{2} (X_{H_u} + X_{H_d}) \quad (35)$$

$$\mathcal{E} = n_g \left(3 \left(\frac{2}{3} \right)^2 X_{H_u} + 3 \left(-\frac{1}{3} \right)^2 X_{H_d} + (-1)^2 X_{H_d} \right) \quad (36)$$

The cosmological Domain Wall (DW) problem can be avoided if $N_{\text{DW}} \equiv 2\mathcal{N} = 1$. $\mathcal{N} = 1/2$ and $N_{\text{DW}} = 1$ can be fulfilled if one family is charged under the PQ symmetry.

Depending on the fermion type, $\tan \theta \in [0.25, 170]$, thus we obtain $\mathcal{E} = 4/3$, $c_u^0 = \cos^2 \theta$, $c_d^0 = \sin^2 \theta$, $c_{N_R}^0 = 1$ from which other couplings including the axion-pion coupling can be determined.

During cosmological first order PTs and bubble evolution processes, three sources for the GW generation have been proposed:

- 1 bubble collision
- 2 sound waves
- 3 magnetohydrodynamic (MHD) turbulence

Gravitational wave signals

The GW energy density spectrum can be characterized by some of important PT quantities including the bubble wall velocity, the released latent heat, and duration of the PT, calculated at the nucleation temperature.

The parameter which is associated with the latent heat:

$$\alpha = \frac{\epsilon}{\frac{\pi^2}{30} g_* T_n^4}, \quad \epsilon = \left(\Delta V_t(T) - T \frac{d\Delta V_t(T)}{dT} \right) \Bigg|_{T=T_n}, \quad (37)$$

There is a critical value of α , denoted by α_∞ , such that for $\alpha > \alpha_\infty$ bubbles can run away

$$\alpha_\infty = \frac{30}{24\pi^2} \frac{\sum_i n_i \Delta m_i^2}{g_* T_n^2}, \quad (38)$$

the inverse of PT duration

$$\frac{\beta}{H_*} = T_n \frac{d}{dT} \left(\frac{S_3(T)}{T} \right) \Bigg|_{T_n}. \quad (39)$$

Gravitational wave signals

In the non-runaway case where $\alpha < \alpha_\infty$, dominant contributions to GWs come from sound waves and MHD turbulence, i.e.,

$$h^2\Omega(f) \simeq h^2\Omega_{\text{sw}} + h^2\Omega_{\text{tu}}$$

$$h^2\Omega_{\text{sw}}(f) = 2.65 \times 10^{-6} \left(\frac{H_*}{\beta}\right) \left(\frac{\kappa_{\text{sw}}\alpha}{1+\alpha}\right)^2 \left(\frac{100}{g_*}\right)^{\frac{1}{3}} v_w S_{\text{sw}}(f), \quad (40)$$

$$h^2\Omega_{\text{tu}}(f) = 3.35 \times 10^{-4} \left(\frac{H_*}{\beta}\right) \left(\frac{\kappa_{\text{tu}}\alpha}{1+\alpha}\right)^{\frac{3}{2}} \left(\frac{100}{g_*}\right)^{\frac{1}{3}} v_w S_{\text{tu}}(f), \quad (41)$$

$$S_{\text{sw}}(f) = \left(\frac{f}{f_{\text{sw}}}\right)^3 \left(\frac{7}{4 + 3\left(\frac{f}{f_{\text{sw}}}\right)^2}\right)^{\frac{7}{2}}, \quad (42)$$

$$S_{\text{tu}}(f) = \frac{\left(\frac{f}{f_{\text{tu}}}\right)^3}{\left(1 + \frac{f}{f_{\text{tu}}}\right)^{\frac{11}{3}} \left(1 + \frac{8\pi f}{h_*}\right)}, \quad (43)$$

Gravitational wave signals

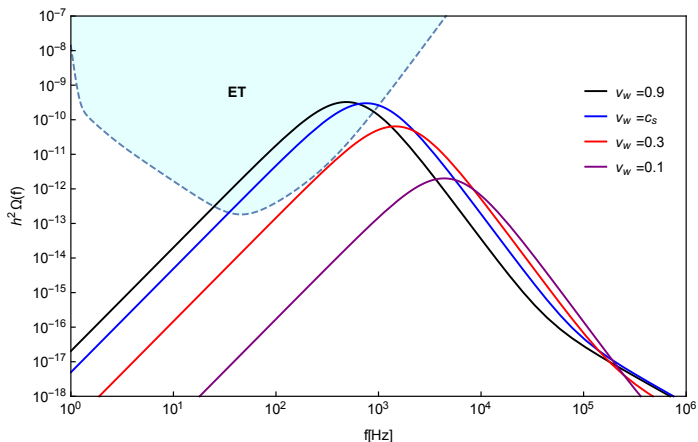


Figure: GW energy density spectra of the first order PQ PT with $f_a = 100$ PeV for different bubble wall velocities and combustion regimes are displayed.

Gravitational wave signals within a heavy axion case

Such class of models can be justified by considering an additional \mathbb{Z}_N mirror symmetry with N mirror worlds, so that with additional confining sectors the axion potential would change, $(a/f_a + \bar{\theta}_{\text{eff}})G_k \tilde{G}_k$. Consequently, in this case the axion mass would be

$$m_a \simeq \frac{\sqrt{z'}}{1+z'} \frac{f_{\pi'} m_{\pi'}}{f_a} \quad (44)$$

in this case the PQ symmetry breaking scale can be $f_a \sim 1 - 100$ TeV. For example taking $z' = z \sim 0.5$, $m_{\pi'} = 135$ GeV, $f_{\pi'} = 93$ GeV and $f_a = 100$ TeV, the axion mass will be $m_a \sim 60$ MeV.

Gravitational wave signals within a heavy axion case

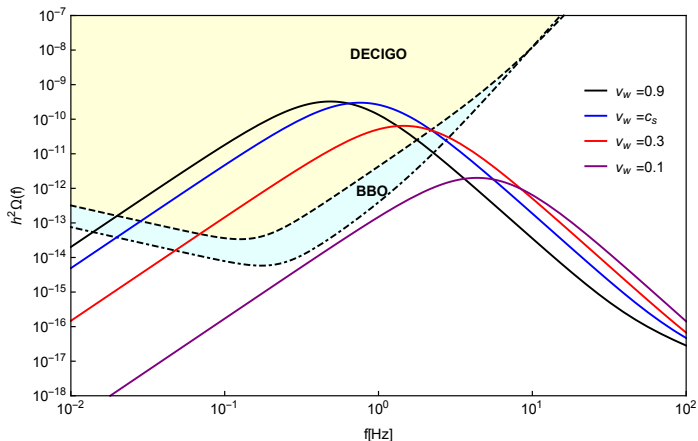


Figure: GW energy density spectra of the first order PQ PT with $f_a = 100$ TeV for different bubble wall velocities are displayed. The signals can be detected by the space-based DECIGO and BBO detectors.

DM-SM neutrino annihilation

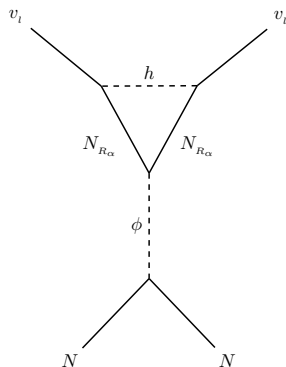


Figure: The DM annihilation to SM neutrinos is shown.

According to the model (Fig. (6)), we consider the annihilation of DM to SM neutrinos $N(p) N(q) \rightarrow \nu_l(k) \nu_l(g)$.

For the non-relativistic DM, $v_D \sim 10^{-3}$, we have $|\mathbf{p}| = |\mathbf{q}| \sim m_N v_D$ and hence the energy of incoming particles $E \sim m_N$. Also, for $m_{\nu_i} \sim 0$ and due to the energy and momentum conservation, $E_{\nu_i} \sim |\mathbf{k}| \sim m_N$. Calculating the amplitude of the process, \mathcal{M} , we can find the cross section

$$\sigma \sim \frac{|\mathbf{k}| |\mathcal{M}|^2}{64\pi E^2 |\mathbf{p}|} \sim 10^{-48} \text{ cm}^2 \left(\frac{\mathcal{Y}}{10^{-2}} \right)^2 \left(\frac{m_N}{1 \text{ PeV}} \right)^{-2} \quad (45)$$

where $\mathcal{Y} \equiv y_1 y_\alpha y_{N_\alpha}^2$ and we take $m_N = y_1 f_a / \sqrt{2} \gg m_\phi$.

Summary

- The bubble filtration mechanism provides a setup which allows DM masses above 100 TeV, the GK bound constrained the DM mass within the thermal freeze-out mechanism.
- an asymmetric DM scenario is proposed during the PQ PT through which DMs can naturally acquire these large masses.
- Based on a QCD axion model extended by chiral neutrinos, the one-loop finite temperature effective potential is found and the PT can be first order within the parameter space of the model.
- The Boltzmann equation is solved and the net number density as well as the observed relic abundance of the DM are obtained. Because of CP violation effects varying during the PT, the scenario is not restricted to $m_N \gg T_n$ for obtaining the relic abundance and also the resulting net abundance remains after the PT.
- The QCD axion couplings are obtained, resolving the strong CP problem in the model.

- The energy density spectrum of GWs generated from the PQ PT for different combustion modes. It is shown the signals can be detected by the future ground-based detectors such as ET.
- the GW signals in the heavy axion case can be explored by DECIGO and BBO detectors.
- Considering the annihilation of DM to SM neutrinos as a source for the PeV-scale neutrinos, the cross section is calculated, consistent with the constraint on DM annihilation processes

Thank You For Your Attention